Aerosol and Air Quality Research, 16: 816–826, 2016

ISSN: 1680-8584 print / 2071-1409 online
doi: 10.4209/aaqr.2015.05.0341

Climatology of New Particle Formation and Corresponding Precursors at Storm Peak Laboratory

A. Gannet Hallar[1*], Ross Petersen[1], Ian B. McCubbin[1], Doug Lowenthal[2], Shanhu Lee[3], Elisabeth Andrews[4,6], Fangqun Yu[5]

[1] *Storm Peak Laboratory, Desert Research Institute, Steamboat Springs, CO, USA*
[2] *Desert Research Institute, Division of Atmospheric Science, Reno, NV, USA*
[3] *University of Alabama in Huntsville, Department of Atmospheric Sciences, Huntsville, Alabama, USA*
[4] *Global Monitoring Division, Earth System Research Laboratory, NOAA, Boulder, Colorado, USA*
[5] *Atmospheric Sciences Research Center, SUNY, Albany, NY, USA*
[6] *Also at Cooperative Institute for Research in Environmental Sciences, University of Colorado, Boulder, Colorado, USA*

ABSTRACT

Thirteen years of measurements of ultrafine (3–10 nm diameter) aerosols are presented from a remote high elevation (3210 m a.s.l.) site in Colorado, Storm Peak Laboratory. Previous work has shown that frequent new particle formation (NPF) occurs regularly at the site (52% of days). This long-term climatology of ultrafine aerosols clearly shows a seasonal dependence on new particle formation at Storm Peak Laboratory, reaching a maximum during the spring season and a minimum in summer. Recent sulfur dioxide data indicates a strong source region west of Storm Peak Laboratory, and this wind direction corresponds to the predominant wind direction observed during NPF events.

Keywords: New particle formation; Mountain site; Sulfur dioxide measurements.

INTRODUCTION

Atmospheric aerosols impact climate, air quality and visibility, and human health (e.g., Akimoto, 2003). Aerosols affect the Earth's radiation balance directly by scattering sunlight and indirectly through their role as cloud condensation nuclei (CCN) (Twomey, 1974; Twomey *et al.*, 1984; Albrecht, 1989; Charlson *et al.*, 1992). Current estimates of aerosol direct and indirect effects remain uncertain because of our inability to accurately estimate the spatial and temporal distributions of aerosol concentrations, size, and composition (Boucher *et al.*, 2013). Radiative effects are primarily related to particles larger than ~50–100 nm, while smaller (< 10 nm) sized particles also have adverse health effects (e.g., Oberdorster *et al.*, 1992; Peters *et al.*, 1997) and are therefore a serious air quality issue.

Aerosol nucleation (formation of aerosol particles directly from gas phase species) is an important atmospheric process that can affect cloud formation. Spracklen *et al.* (2010) showed that a global aerosol microphysics model was unable to reproduce the observed annual cycles in aerosol number concentrations if nucleation was not included. Merikanto *et al.* (2009) and Yu and Luo (2009) showed that aerosol nucleation can indeed have a great impact on the number of the global CCN. A global study showed that nucleation in the free troposphere contributes to 35% of CCN that forms low -level clouds at supersaturation ratio of water of 0.2% (Merikanto *et al.*, 2009). In general, the contribution of primary particles to CCN decreases at higher elevations with respect to the contribution from nucleation (Merikanto *et al.*, 2009). Model results by Yu and Luo (2009) showed that secondary particles formed via nucleation in sub-grid SO_2 plumes contribute up to 50–70% of CCN. These results suggest that high altitude NPF can play a critical role in cloud formation and hence climate.

NPF AT MOUNTAIN SITES

There are several potential underlying principles that allow nucleation to occur more frequently at high elevations. First, increased levels of ultra-violet (UV) radiation have been associated with NPF. Previous studies have shown that increased UV irradiance is associated with increased atmospheric OH radical concentrations, which drive the formation of sulfuric acid, a key chemical species known to be involved in aerosol nucleation (e.g., Berndt *et al.*, 2005). Most recently, NPF data from Storm Peak Laboratory (SPL) was used within a global chemical transport model to

* Corresponding author.
Tel.: 1-970-819-0968; Fax: 1-970-870-7914
E-mail address: gannet.hallar@dri.edu

illustrate the critical role that sulfuric acid plays in the initial nucleation process (Yu and Hallar, 2014). Increased radiation may also allow for increased plant production and emissions of biogenic volatile organic compounds (BVOC) (e.g., Guenther *et al.*, 2006), which potentially impact nucleation and provide condensable species needed for particle growth (Bonn *et al.*, 2008). Previous measurements at SPL, showed higher level of UV irradiance on days with identified NPF, compared with days without these events (Hallar *et al.*, 2011). NPF events were also correlated with UV radiation during a one-year study at Jungfraujoch in the Swiss Alps (3580 m a.s.l.) (Boulon *et al.*, 2010). Secondly, high elevations tend to have lower temperatures and lower surface area of pre-existing aerosol particles than at lower elevations. Nucleation is a non-linear process and temperature is a key thermodynamic parameter (Yu, 2010). At sufficiently low temperatures, it is even possible that the nucleation barrier can disappear and nucleation can take place spontaneously (Yu, 2010). On the other hand, pre-existing aerosol surface area is a sink for nucleation; since nucleation precursors preferentially condense on larger aerosols and newly formed small particles will quickly coagulate with large particles (Kulmala, 2003). Thus, lower temperature and lower surface area of aerosol particles, together with higher precursor concentrations due to convection and enhanced irradiance, can create excellent conditions for nucleation at high elevations.

Additionally, high elevations may provide a favorable thermodynamic condition for NPF due to turbulence, atmospheric waves, storms, and other air mixing processes (e.g., Nilsson and Kulmala, 1998). Turbulence on various scales including the presence of boundary layer turbulence (Nilsson *et al.*, 2001), atmospheric waves (Nilsson *et al.*, 2000), and mixing across temperature and humidity gradients (Kulmala *et al.*, 1998) may promote nucleation. These mixing conditions can create higher supersaturation ratios of nucleation precursors. Recent evidence also supports the role of turbulence in NPF (Wehner *et al.*, 2010). NPF may be also promoted by smaller-scale turbulence associated with surface friction in orographic flow at high elevation ground locations (Boulon *et al.*, 2011).

Measurements above the boundary layer are needed to evaluate the global effects of aerosols on climate. The only high-altitude measurement approach that allows for continuous, long-term observations is the use of mountaintop laboratories (Weber *et al.*, 1995). Using two different high altitude sites, the Puy de Dôme research station (1465 m a.s.l.) and the Opme Station (660 m a.s.l.) in central France, a recent study illustrated the importance of vertical extent for nucleation events (Boulon *et al.*, 2011). At this station Boulon *et al.* (2011) found a NPF frequency of 36% during a 157-day study, and the NPF frequency was greater (36%) at the higher elevation site compared to the lower elevation site (21%). Using LIDAR measurements, this work highlighted that NPF occurs frequently above the boundary layer and supports the conclusion that nucleation is promoted at high elevations (Venzac *et al.*, 2008). At Jungfraujoch, aerosol nucleation was found on 18% of the 226 measurement days from 2008 to 2009 (Boulon *et al.*, 2010). Venzac *et al.* (2008) reported a nucleation frequency of 35% during a 511-day study at the Nepal Climate Observatory (5,079 m a.s.l.). Neitola *et al.* (2011) reported four years of measurements from Mukteshwar in the Himalaya foothills (2180m a.s.l.), where the highest daily NPF frequency was found during the spring (with over 80% of all events), and overall NPF occurred 14.5% of days. García *et al.* (2014) presented a four-year data set from Izaña Mountain (2373 m a.s.l.) in the North Atlantic demonstrating NPF on 30% of days. There was a clearly marked NPF season at Izaña in the summer (May to August), where events accounted for 50–60% of the days. Most recently, Rose *et al.* (2015) presented one-year of data from highest in-situ aerosol measurement site in the world, Chacaltaya (5240 m a.s.l.), Bolivia. This site showed remarkably high NPF frequency of 64%, with a clear seasonal dependence. NPF was found primarily in the dry season (May–October), and commonly multiple events were identified per day. Overall, the seasonality of NPF at high elevation sites varies significantly with local conditions.

Frequent NPF has been observed regularly at Storm Peak Laboratory. These events occurred during 52% of the 474 measurement days from 2001 to 2009 (Hallar *et al.*, 2011). This work uses a long-term record of ultrafine aerosol concentration to determine the seasonality of NPF at Storm Peak Laboratory, and consider local precursors of aerosol nucleation.

METHODOLOGY

Location

Storm Peak Laboratory (SPL, 3210 m a.s.l.; 40.455°N, 106.745°W), operated by the Desert Research Institute (DRI), is located on the west summit of Mt. Werner in the Park Range near Steamboat Springs in northwestern Colorado. This site has been used in cloud and aerosol studies for more than 25 years (e.g., Borys and Wetzel, 1997; Lowenthal *et al.*, 2002). SPL is situated at treeline on a 70 km ridge oriented perpendicular to the prevailing westerly winds. SPL is 1120 meters above the nearest population center; at this mountain-top remote location studies of the long-term trends aerosol properties have been made (e.g., Asmi *et al.*, 2013).

Methods

Meteorological Data

Meteorological instruments used in this study include research grade temperature, pressure, wind speed and direction, and relative humidity sensors (Campbell Scientific, Inc., Met One and Vaisala). These data are uploaded to the Western Regional Climate Center (http://www.wrcc.dri.edu/) database every 5 min.

Aerosol Data

Particles were sampled from an insulated, six-inch diameter manifold within four feet of its horizontal entry point through an outside wall. The 4 m high vertical section outside the building is capped with an inverted can to exclude large particles (D > ~8 μm) as well as rain and precipitation.

Aerosol size distributions were measured with a TSI SMPS 3936L22 (scanning mobility particle sizer with a TSI 3022 CPC) for particles with diameters between 8 and 330 nm, and with a nano-SMPS (TSI 3936N76 with a TSI 3776 CPC) for particles with diameters between 3 and 96 nm. For the nano-SMPS and the SMPS, sheath and sample flow rates were 10 L min^{-1} and 1 L min^{-1}, respectively. All SMPS and nano-SMPS distributions were corrected for multiple-charge and diffusional losses. Five-minute scans were collected from the SMPS and nano-SMPS. The SMPS dataset started in 2001, although is not continuous. The nano-SMPS data set was collected from December 2010–April 2011. Long-term SMPS data from SPL is primarily available from the spring and winter months, with a smaller dataset representing the summer months. Due to limited access to SPL, combined with measurement complexity, very little long-term SMPS data is currently available representing the fall season. For this study, non-continuous data from April 3, 2013 to July 12, 2014 are presented in detail, as this period overlaps with new measurements of sulfur dioxide (discussed below). This subset of SMPS data primarily represents the winter season (61% of available data) and summer season (28% of available data). The fall season represents only 10% of the available data, and the spring season represents less than 1% of the available data (due to an instrument failure).

Condensation nucleus (CN) concentrations were measured with TSI 3025 and 3010 condensation particle counters (CPC) for particles with diameters greater than 3 and 10 nm, respectively. Concentrations of ultrafine particles (UFCN) were determined by the difference. CN concentrations were averaged and recorded every five minutes, prior to 2011. After 2011, the CN concentrations were averaged and recorded ever minute. SPL has one of the longest records of aerosol number concentration in North America (Asmi *et al.*, 2013). The TSI 3010 CN concentration records started in 1998 and the TSI 3025 CN concentration record started in 2001. The quality assurance protocol for a Global Atmospheric Watch (GAW) station was adapted for this dataset. All data were collected and then meticulously pre-screened by SPL staff prior to generation of the final quality controlled data set. Local contamination sources (e.g., snowmobiles and snow cat passing SPL during the ski season) were removed from the final data set. The historical CN data from SPL were incorporated into the aerosol database archive of National Oceanic and Atmospheric Administration Global Monitoring Division's (NOAA/GMD) Aerosol Group when SPL joined NOAA/GMD's collaborative aerosol network. In sum, TSI 3010 data at SPL is available from 1998-2012 with nearly continuous coverage (Asmi *et al.*, 2013; Fig. 2), and the TSI 3010 has continued monitoring CN concentration uninterrupted since 2012. TSI 3025 data is available from 2001–2007 and from 2009–2014, and thus this is the timeframe used in this study. Hourly averaged CN and UFCN data are used in this study.

Sulfur Dioxide Data

Measurements of sulfur dioxide were made using a Thermo Scientific Trace level sulfur dioxide (SO_2) instrument (Model 43iTLE). The Air Pollution Control Division of Colorado Department of Public Health and the Environment performs an audit of this instrument annually. As suggested by the Quality Assurance Handbook for Air Pollution Measurement Systems, published by the U.S. EPA, 2006, the SO_2 instruments is calibrated daily with zero air and a NIST-traceable primary standard. The SO_2 data record spans the time range from March 28, 2013 to August 11, 2014. Unlike the SMPS, the sulfur dioxide instrument ran nearly continuously during this timeframe. Thus, all seasons are well represented. The spring and summer season each covering approximately 30% of the data. Both the fall and winter season represented approximately 20% of the total dataset.

RESULTS

Previous studies (Hallar *et al.*, 2011; Yu and Hallar, 2014) have used aerosol size distribution data to study NPF at SPL. This work has clearly established that NPF is frequent at the site, during the daytime. As demonstrated in the prior publications (Hallar *et al.*, 2011; Yu and Hallar, 2014) and in Fig. 1 below, these events are clearly distinguishable in both the nano-SMPS and standard SMPS data. Unfortunately, the size distribution data is not continuous, and thus cannot provide a seasonal climatology of NPF.

The seasonal average and one standard deviation of aerosol concentration with diameters greater than 3 and 10 nm are shown in Table 1. Each season is defined as follows: Spring is March, April and May; Summer is June, July, and August; Fall is September, October, and November; Winter is December, January, and February both in Table 1 and for the remainder of this paper. There is no statistically significant seasonal trend in aerosol concentration at SPL, either in the CN concentration or the UFCN concentration, although concentrations of UFCN may be higher in the spring.

Table 1 also shows the meteorological climatology at SPL. Monthly averaged data from September 1992–December 2014 were used to create the seasonal averages, shown in Table 1. The site is consistently impacted by wind from the West, across all seasons. Consistent with a Northern Hemisphere high alpine location, SPL experiences a large temperature span between winter and summer. The fall and spring seasons have a similar temperature profile.

Previous work (Hallar *et al.*, 2011) used 474 measurement days from 2001 to 2009 and calculated an average initiation time for NPF events at SPL. The initiation time of the event on each day was defined if the concentration of particles within the first three SMPS size bins (diameter midpoint between 8–10 nm) was above 47 cm^{-3} or 3000 in units of dN/dlogDp. The average initiation time for NPF events was 12:11 ± 99 min. No nighttime events were observed at SPL (Hallar *et al.*, 2011). As mentioned in introduction, NPF was found 52% of days at SPL during the timeframe of the Hallar *et al.* (2011) study.

NPF events can also be identified by considering the difference between the 3010 CPC and 3025 CPC during daytime and nighttime hours. Because these instruments operated more continuously than the SMPS's they can also

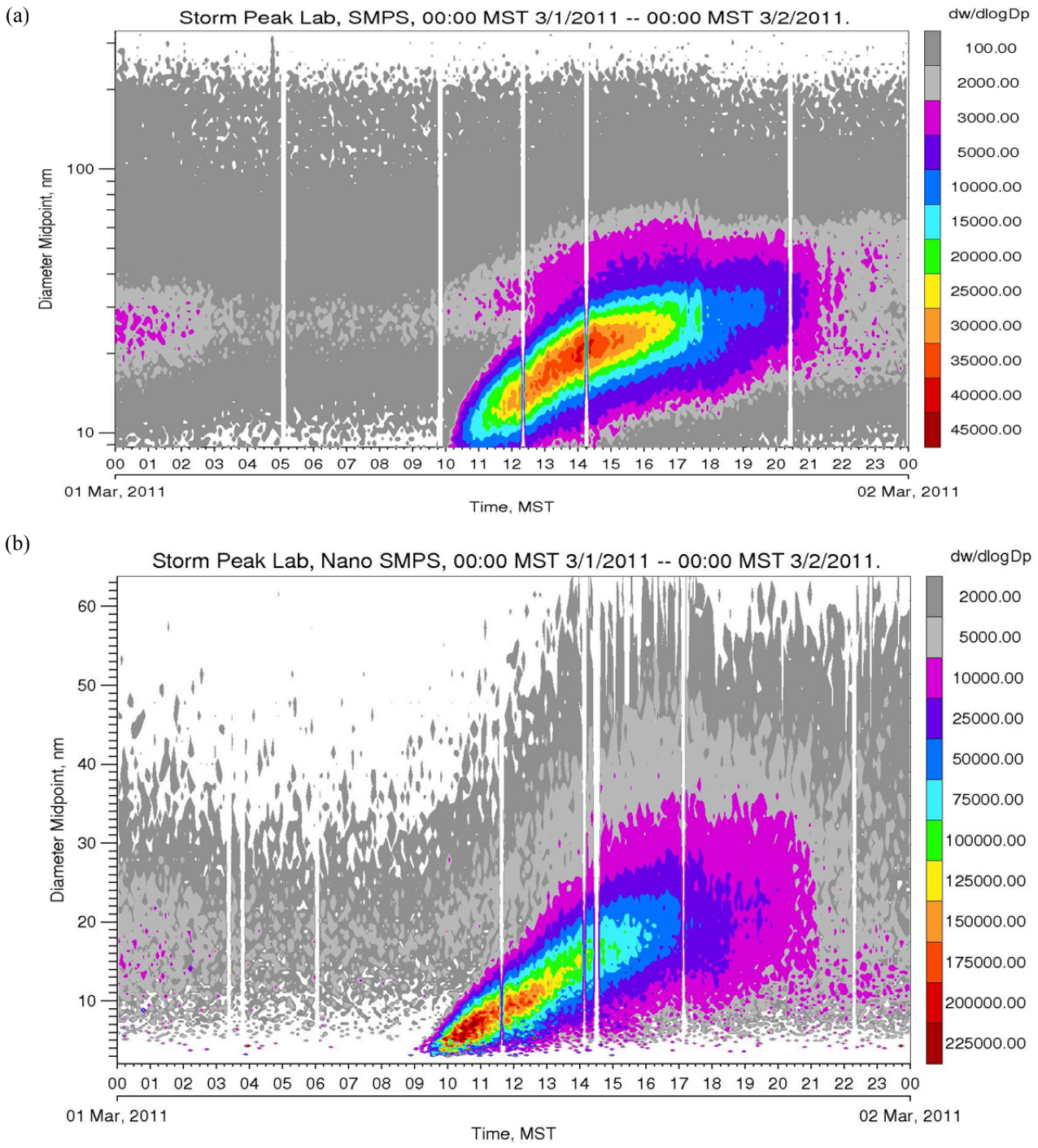

Fig. 1. Particle size distributions are presented as a concentration matrix, with the x-axis representing time and the y-axis representing the particle size and the colors represents the concentration. Concentrations are reported in units of dN/dlogDp. Fig. 1(a) presents data from the standard SMPS at SPL from one day, March 1, 2011. Fig. 1(b) presents nano-SMPS data for the same time period at SPL.

Table 1. Seasonality of CN concentration (# cm^{-3}) and meteorological variables.

Season	Mean TSI 3010	SD TSI 3010	Mean TSI 3025	SD TSI 3025	Mean Wind Dir. (°)	SD Wind Dir. (°)	Mean Temp (C)	SD Temp (C)
Spring	2322	1980	3082	2566	261	22	-2.2	4.2
Summer	1945	1615	2811	2173	250	38	11.8	2.8
Fall	1518	1377	2204	1987	259	38	0.3	7.4
Winter	1735	1580	2294	2082	264	37	-9.8	1.8

provide a means of detecting a seasonal pattern in NPF. The method consists of observing the "difference of differences". First the difference between the 3025 CPC and the 3010 CPC was taken to find the concentration of particles between 3 and 10 nm, for daytime and nighttime, as shown in Fig. 2. This figure highlights the seasonality of ultrafine aerosol concentration at SPL. Nighttime values show a maximum in the summer season and a minimum in the winter. Next, the nighttime difference (no NPF) was subtracted from the daytime difference (indicating NPF). This separation into daytime and nighttime was performed for the time intervals 8 am to 4 pm and 11 pm to 4 am, respectively, based on Hallar *et al.* (2011). The resulting values, shown as a monthly average spanning from 2001 to 2007 and 2009–2014 in Fig. 3, clearly displays seasonality in NPF. The maximum of NPF occurs in March, while the three lowest NPF months are May through July. A second smaller peak of NPF is observed in the fall season, with a maximum in October. In general the number of NPF events was highest during the spring (March) followed by the fall (September–November), then winter (Dec–Jan–Feb) and finally a strong decrease was found in the summer (May–June–July). There are limitations to this technique; primarily that it is not a direct observation of particle growth (i.e. banana curves are not observed).

Using the available SO_2 dataset, in conjunction with the meteorology data, source regions or geographic areas of this nucleation precursor were considered. To specifically investigate sources of SO_2, only time periods with SO_2 events were considered. An event was defined when the SO_2 concentration was above 0.5 ppb, and events were found in 11% of the dataset. Fig. 4(a) demonstrates the wind direction and wind speed during the timeframe where SO_2 data was available (March 2013 to August 2014). The wind direction primarily spans from 200° to 315°, with wind speeds typically below 20 m s^{-1}. Fig. 4(b) demonstrates the wind direction and SO_2 concentration for events. The SO_2 events are primarily found in a narrower wind direction range, between 265° and 305°, suggesting a specific source region for SO_2 at SPL. Hallar *et al.* (2011; their Fig. 3) previously demonstrated that NPF events at SPL correspond more closely to a westerly wind direction, specifically the wind direction spanning from 255° to 305°.

Table 2 displays the seasonal averaged SO_2 concentration for the entire dataset, events greater than 0.2 ppb, and events greater than 0.5 ppb. The standard deviation and the 95% confidence interval (calculated from a normal distribution) of the mean are also shown. During the summer months, there is a statistically significant lower SO_2 concentration found using the entire dataset. When considering only events where the SO_2 concentration is greater than 0.2 ppb or 0.5 ppb, the highest concentration is consistently found during the spring months, and the lowest concentration is found in the summer months. These seasonal trends in SO_2 concentration demonstrate strong statistical significance. Again, events with SO_2 concentrations above 0.5 ppb are found in 11% of the overall dataset, but they are only found during 5% of the summertime. Thus the seasonal pattern of the NPF is consistent with the seasonality of SO_2 concentration, i.e., the maximum is found in the spring and the minimum is found in the summer.

In order to identify a potential source region, the spring

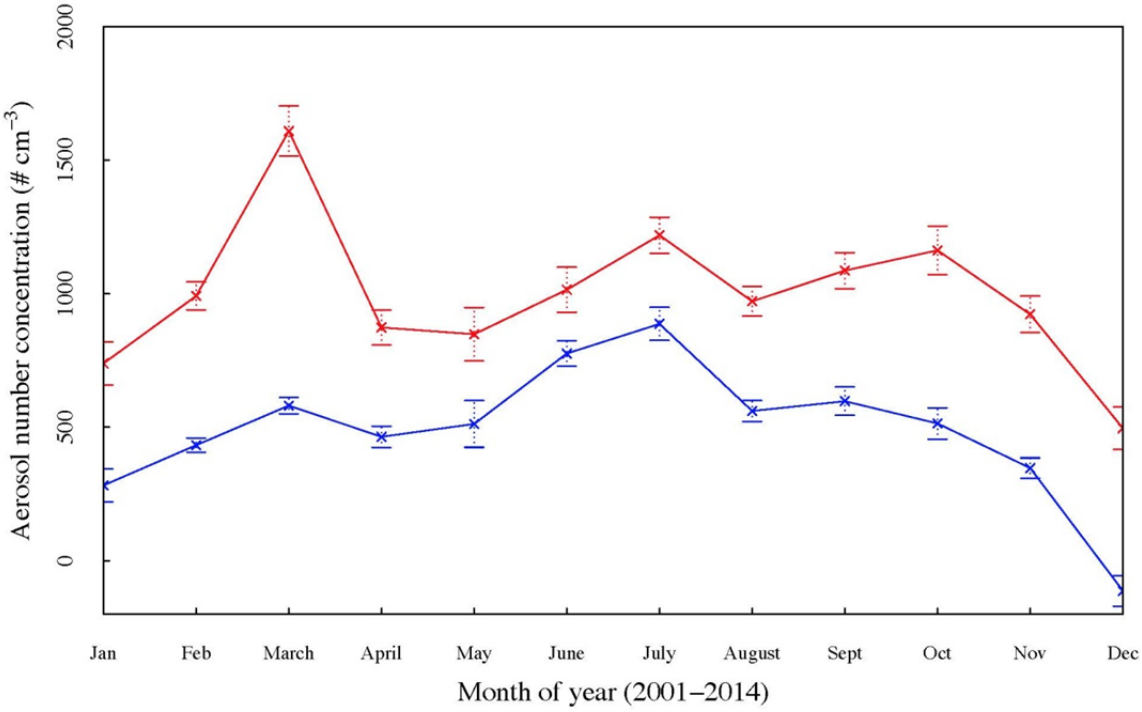

Fig. 2. Monthly averages showing the difference between the 3025 CPC and the 3010 CPC to find the concentration of particles between 3 and 10 nm. Nighttime difference is shown in blue, and daytime difference is shown in red. Standard deviations are shown with the vertical bars.

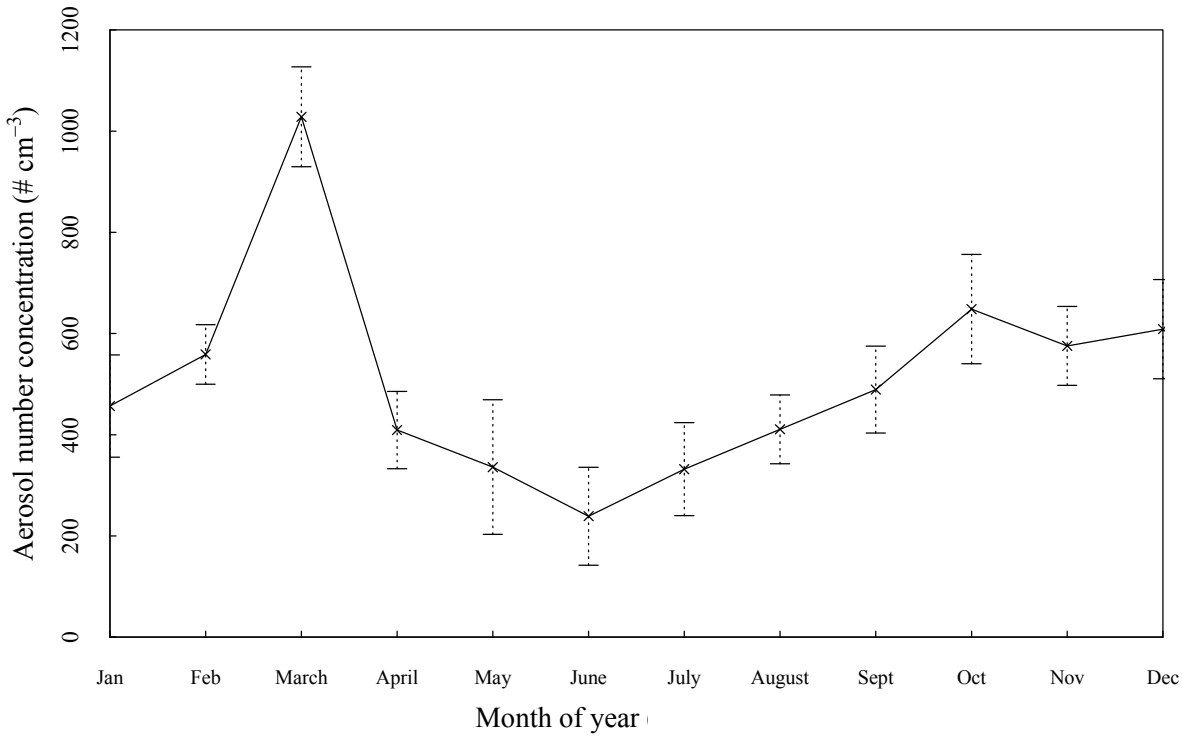

Fig. 3. Monthly averages showing the "difference of the difference". First, the difference between the 3025 CPC and the 3010 CPC was taken to find the concentration of particles between 3 and 10 nm, then nighttime difference (no NPF) was subtracted from the daytime difference (indicating NPF). Standard error bars calculated from the daily measurements within each month are shown.

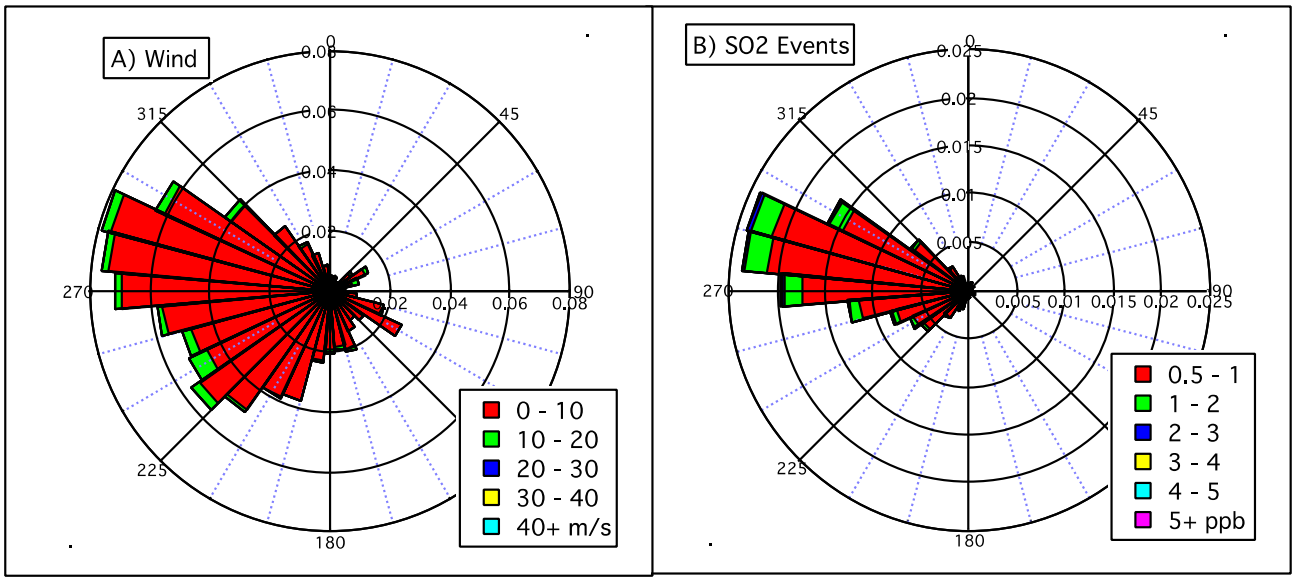

Fig. 4. A) SPL Wind Rose from 3/28/2013 to 8/11/2014; B) Wind rose showing SO_2 concentration for events with SO_2 greater than 0.5ppb. Colors demonstrate SO_2 concentration. Radius indicates probability.

and summer seasonality of SO_2 events (SO_2 > 0.5 ppb) are further compared in Figs. 5(a) and 5(b). As illustrated with the averages shown in Table 2, there is a greater probability of finding high concentrations of SO_2 in the spring. Similar to the climatological patterns displayed in Fig. 4, the springtime SO_2 events clearly show a wind direction representing a source region originating in a narrower region, typically from the wind directions between 265° to 295°. In the summertime the wind direction shows more variation during the SO_2 events. There is also a higher probability of having a Westerly (265° to 295°) wind direction in the spring season than the summer.

Table 2. Seasonality of SO_2 concentration for all data and as a function of event constraints.

	Average	Standard Deviation	95% confidence	% of Data
All				
Spring	0.23	0.77	0.005	100
Summer	0.15	0.20	0.001	100
Fall	0.22	0.46	0.004	100
Winter	0.23	0.47	0.004	100
Events > 0.2 ppb				
Spring	0.65	1.39	0.006	27
Summer	0.43	0.29	0.004	21
Fall	0.59	0.73	0.004	29
Winter	0.60	0.74	0.012	30
Events >0.5 ppb				
Spring	1.28	2.23	0.047	9
Summer	0.78	0.37	0.011	5
Fall	1.00	1.01	0.026	12
Winter	1.01	1.01	0.025	12

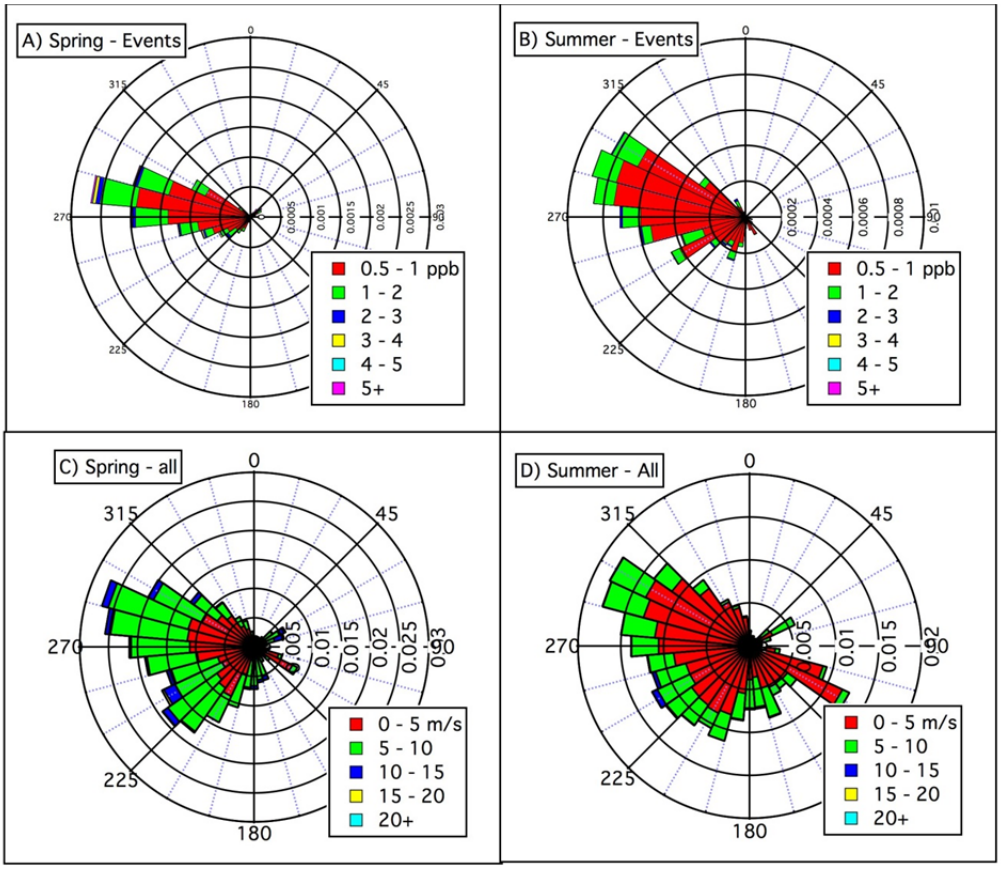

Fig. 5. A) Wind rose showing SO_2 events and wind direction for spring data (from 3/28/2013–5/31/2013 and to 3/1/2014–5/31/2014. Radius demonstrates probability, and color demonstrates SO_2 concentration. B) Same as A for summer (6/1/2013–8/30/2013 and 6/1/2014–8/11/2014). C) Wind rose showing wind direction from SPL, with color demonstrating wind speed for spring dates. D) Same as C for summer dates.

Finally, time periods were evaluated when both SMPS and SO_2 data were available (i.e., the non continuous dataset from 4/3/2013 to 7/12/2014). As indicated earlier, this dataset is biased towards the winter season (winter represents 61% of the combined SMPS and SO_2 data set). Within the time period of April 2013 to July 2014, there is a stronger probability of having a Westerly (265° to 295°) wind direction in the winter season in comparison to the entire data set (Figure not shown). The three datasets (SMPS, SO_2, and Meteorological) were merged into 15-minute averages. Fig. 6(a) demonstrates all wind directions sampled, when SMPS data was available. While wind directions

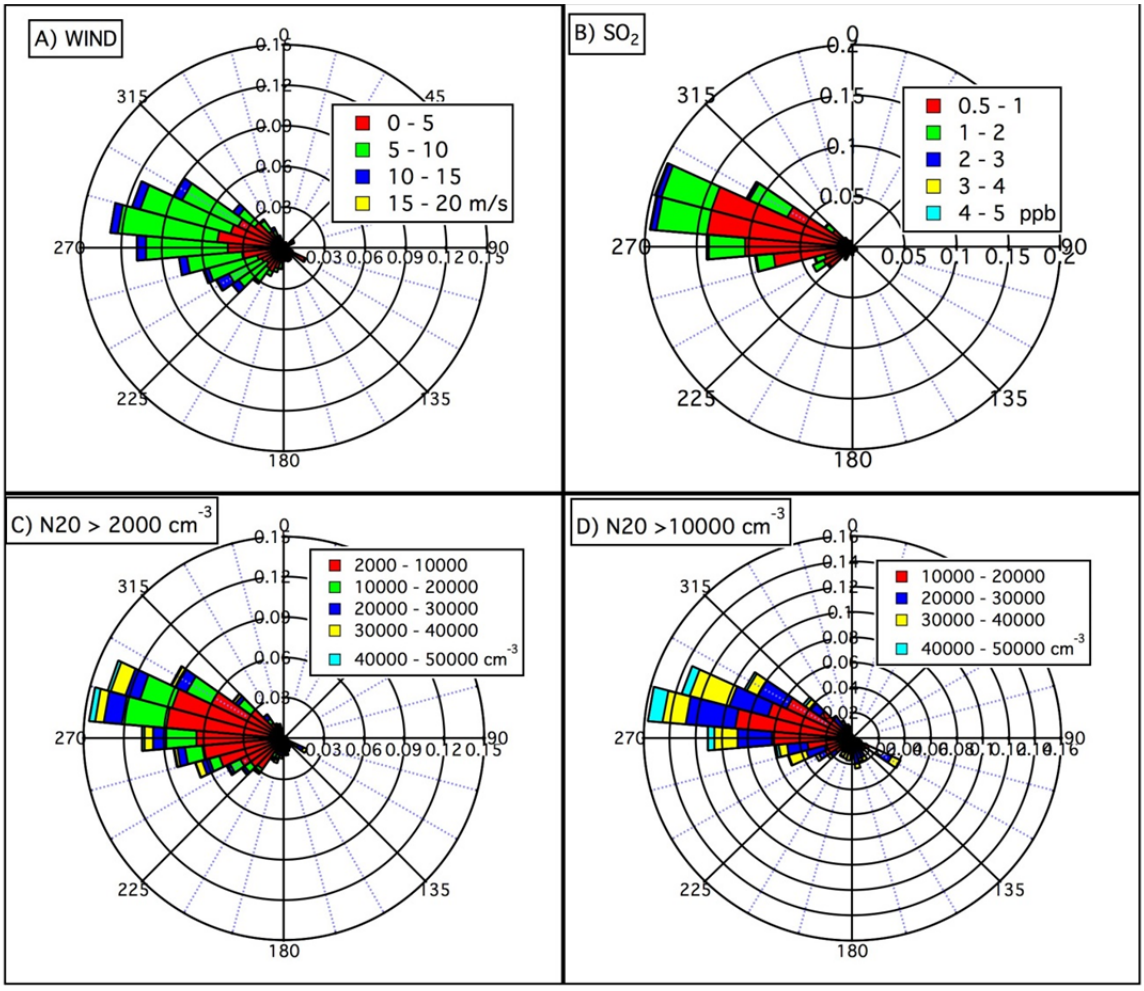

Fig. 6. A) SPL Wind rose from 4/3/2013 to 7/12/2014, when both SMPS and SO_2 data were available; B) Wind rose showing SO_2 concentration for events with SO_2 greater than 0.5 ppb. Colors demonstrate SO_2 concentration. C) Wind rose showing SMPS concentration for particles smaller than 20 nm (N20) when concentration of N20 is greater than 2000 cm^{-3}. Colors demonstrate aerosol concentration for particles smaller than 20 nm. D) Wind rose showing N20 concentration only for events when concentration of N20 is greater than 10000 cm^{-3}. Colors demonstrate aerosol concentration for particles smaller than 20 nm. For all four plots in this figure the radius indicates probability.

were measured in all quadrants at SPL, the dominant wind direction is found primarily in the Westerly sector, between 220° to 305°.

Subsequently, the wind direction was considered for events during this timeframe when the SO_2 measurement was greater than 0.5 ppb. This criterion significantly narrows the wind direction sampled. Specifically, SO_2 events were only sampled when the wind direction was within a subset of the Westerly sector, primarily between 265° to 305°, as shown in Fig. 6(b). To evaluate the occurrence of NPF during this timeframe using SMPS data, the first 22 channels of the SMPS data were summed to calculate the concentration of particles smaller than 20 nm (N_{20}). Two thresholds were considered representing all NPF (N_{20} > 2000 cm^{-3}) and strong NPF events (N_{20} > 10000 cm^{-3}). It is important to note that this methodology may also include pollution events, which impact particle concentrations below 20 nm. From our visual inspection of the SMPS data, pollution events, which look much different than NPF events (i.e., lack of a distinct diurnal pattern), are a rare occurrence. Fig. 6(c) is a wind rose plot showing SMPS concentration when the concentration of N_{20} is greater than 2000 cm^{-3}. Similar to the SO_2 > 0.5 ppb requirement of an SO_2 event, this N_{20} >2000 cm^{-3} criterion also narrows the wind direction sampled. Specifically, NPF events were only observed when the wind direction was within a subset of the Westerly sector, again primarily between 265° to 305°. When the criterion is further strengthened to N_{20} > 10000 cm^{-3}, representing strong NPF events, the observed wind directions narrow even further (Fig. 6(d)). The probability, indicated by radii on Figs. 6(c) and 6(d), of finding a strong NPF event (N_{20} > 10000 cm^{-3}) increased slightly from 265° to 305°, in comparison to all NPF (N_{20} > 2000 cm^{-3}).

DISCUSSION AND CONCLUSIONS

Northern hemisphere atmospheric observations in general have shown the highest NPF frequency in the spring,

similar to the measurements presented here. A high seasonal event frequency in spring in the northern hemisphere is shared by other statistical descriptions of NPF events across the globe (e.g., Birmili and Wiedensohler, 2000; Hõrrak *et al.*, 2000; Mäkelä *et al.*, 2000; Birmili *et al.*, 2003; Dal Maso *et al.*, 2005; Pryor *et al.*, 2010). There are a few exceptions to this seasonal trend found in the literature, including the high elevations studies discussed in the introduction. Additionally, Jaatinen *et al.* (2009) found a high NPF frequency in the summer at San Pietro Capofiume, in the Po Valley of Italy, and a high NPF in the fall in Melpitz, Germany. Both of these low elevation locations are strongly urban influenced. More similar to the measurements here, Kanawade *et al.* (2012) and Stanier *et al.* (2004) found a high frequency of NPF in both the spring and fall, and this was usually associated with elevated SO_2 concentrations. These two studies represented semi-rural continental (Kent, Ohio) and urban (Pittsburgh, Pennsylvania) environments respectively. To our knowledge, this is the first study reporting a high frequency of NPF in both the spring and fall in a remote, high elevation location.

The observed seasonality of NPF at SPL is consistent with chemical composition data observed during short field campaigns at the site. Friedman *et al.* (2013) reported single particle composition (size range: 0.05–3 μm) measured at SPL in March 2011, and showed that sulfate with a small amount of organics was the dominant particle class. In contrast, Hallar *et al.* (2013) showed that organic compounds (OC) compose the majority (~64%) of the mass of particles collected with filters at SPL in July 2010. The dominance of SPL particle mass by sulfate in March and by OC in July provides a contrast during different seasons: sulfate-rich spring and organics-rich summer. Previous model simulations of aerosol chemistry at SPL indicate that condensable aerosol precursors were dominated by H_2SO_4 in March and by low volatile secondary organic gases (LV-SOGs) in July (Yu and Hallar, 2014), and that H_2SO_4 plays a much more important role in the initial nucleation process. Since NPF formation is strongly dependent on H_2SO_4 and temperature (Yu, 2010), the high frequency of NPF in both the spring and fall observed at SPL is likely a result of combined effects of seasonal variations in key parameters including SO_2 concentrations. Previous work at SPL also has shown that NPF is associated with increased UV flux and a low surface area of pre-existing particles (Hallar *et al.*, 2011).

The combined results have interesting implications for nucleation processes, i.e., key parameters controlling NPF in the remote atmosphere. The difference between the general wind direction at SPL, and the wind direction with high concentrations of SO_2 and NPF (shown in Figs. 4, 5 and 6) suggest a specific source region. Three coal-fired power plants are located directly to the west of SPL, at distances of approximately 50, 80, and 250 km, proving ample year-round SO_2. Previous research (e.g., Borys *et al.*, 2000; Hallar *et al.*, 2013; Zhao *et al.*, 2013) has also noted the potential of these power plants to influence aerosol properties and cloud microphysics at SPL. Data from SPL continues to suggest strong implications for the role of H_2SO_4, stemming from SO_2 emitted by coal fired power plants, on the aerosol number concentration and size distribution in remote areas. These data can also be used to evaluate various nucleation theories as well as the performance of regional and global aerosol models.

ACKNOWLEDGEMENTS

The authors appreciate the dedication, commitment, and effort of Randolph Borys, and Peter Atkins towards the long-term measurements of aerosol concentration at Storm Peak Laboratory (SPL). Instrumentation at SPL used in this analysis was purchased via a grant AGS-0079486 and AGS-1040085 from the US National Science Foundation. The authors appreciate the assistance from the Colorado Department of Public Health and Environment Air Pollution Control Division/Technical Services Program with the installation and calibration of trace gas monitors at SPL. We appreciate the support of NOAA's Global Monitoring Division's Aerosol Group for ingesting the CN data to a consistent data structure for archive and availability. Thank you to Galina Chirokova for programming efforts. The Steamboat Ski Resort provided logistical support and in-kind donations. The Desert Research Institute is a permittee of the Medicine-Bow Routt National Forests and is an equal opportunity service provider and employer.

REFERENCES

Akimoto, H. (2003). Global Air Quality and Pollution. *Science* 2003. 302: 1716–1719.

Albrecht, B.A. (1989). Aerosols, Clouds, Microphysics, and Fractional Cloudiness. *Science* 245: 1227–1230.

Asmi, A., Collaud Coen, M., Ogren, J.A., Andrews, E., Sheridan, P., Jefferson, A., Weingartner, E., Baltensperger, U., Bukowiecki, N., Lihavainen, H., Kivekäs, N., Asmi, E., Aalto, P.P., Kulmala, M., Wiedensohler, A., Birmili, W., Hamed, A., O'Dowd, C., G Jennings, S., Weller, R., Flentje, H., Fjaeraa, A.M., Fiebig, M., Myhre, C.L., Hallar, A.G., Swietlicki, E., Kristensson, A. and Laj, P. (2013). Aerosol Decadal Trends – Part 2: In-situ Aerosol Particle Number Concentrations at GAW and ACTRIS Stations. *Atmos. Chem. Phys.* 13: 895–916, doi: 10.5194/acp-13-895-2013.

Berndt, T., Böge, O., Stratmann, F., Heintzenberg, J. and Kulmala, M. (2005). Rapid Formation of Sulfuric Acid Particles at near-Atmospheric Conditions. *Science* 307: 698–700.

Birmili, W. and Wiedensohler, A. (2000). New Particle Formation in the Continental Boundary Layer: Meteorological and Gas Phase Parameter Influence, *Geophys. Res. Lett.* 27: 3325–3328.

Birmili, W.H., Berresheim, H., Plass-Dulmer, C., Elste, T., Gilge, S., Wiedensohler, A. and Uhrner, U. (2003). The Hohenpeissenberg Aerosol Formation Experiments (HAFEX): A Long-term Study Including Size-resolved Aerosol, H_2SO_4, OH, and Monoterpenes Measurements. *Atmos. Chem. Phys.* 3: 361–376.

Bonn, B., Kulmala, M., Riipinen, I., Sihto, S.L. and Ruuskanen, T. (2008). How Biogenic Terpenes Govern

the Correlation between Sulfuric Acid Concentrations and New Particle Formation. *J. Geophys. Res.* 113: D12209.

Borys, R.D. and Wetzel, M.A. (1997). Storm Peak Laboratory: A Research, Teaching, and Service Facility for the Atmospheric Sciences. *Bull. Am. Meteorol. Soc.* 78: 2115–2123.

Borys, R.D., Lowenthal, D.H. and Mitchell, D.L. (2000). The Relationships among Cloud Microphysics, Chemistry, and Precipitation Rate in Cold Mountain Clouds. *Atmos. Environ.* 34: 2593–2602.

Boucher, O., Randall, D., Artaxo, P., Bretherton, C., Feingold, G., Forster, P., Kerminen, V.M., Kondo, Y., Liao, H., Lohmann, U., Rasch, P., Satheesh, S.K., Sherwood, S., Stevens, B. and Zhang, X.Y. (2013). Clouds and Aerosols. In *Climate Change 2013: The Physical Science Basis. Contribution of Working Group I to the Fifth Assessment Report of the Intergovernmental Panel on Climate Change*, Stocker, T.F., Qin, D., Plattner, G.K., Tignor, M., Allen, S.K., Boschung, J., Nauels, A., Xia, Y., Bex, V. and Midgley, P.M. (Eds.), Cambridge University Press, Cambridge, United Kingdom and New York, NY, USA.

Boulon, J., Sellegri, K., Venzac, H., Picard, D., Weingartner, E., Wehrle, G., Collaud Coen, M., Bütikofer, R., Flückiger, E., Baltensperger, U. and Laj, P. (2010). New Particle Formation and Ultrafine Charged Aerosol Climatology at a High Altitude Site in the Alps (Jungfraujoch, 3580 m a.s.l., Switzerland). *Atmos. Chem. Phys.* 10: 9333–9349.

Boulon, J., Sellegri, K., Hervo, M., Picard, D., Pichon, J.M., Fréville, P. and Laj, P. (2011). Investigation of Nucleation Events Vertical Extent: A Long Term Study at Two Different Altitude Sites. *Atmos. Chem. Phys.* 2011. 11: 5625–5639.

Charlson, R.J., Schwartz, S.E., Hales, J.M., Cess, R.D., Coakley, J.A., Jr., Hansen, J.E. and Hofmann, D.J. (1992). Climate Forcing by Anthropogenic Aerosols. *Science* 255: 423–430.

Dal Maso, M., Kulmala, M., Riipinen, I., Wagner, R., Hussein, T., Aalto, P. and Lehtinen, E.J. (2005). Formation and Growth Rates of Fresh Atmospheric Aerosols: Eight Years of Aerosol Size Distribution Data from SMEARII, Hyytiälä, Finland. *Boreal Environ. Res.* 10: 323–336.

Friedman, B., Zelenyuk, A., Beranek, J., Kulkarni, G., Pekour, M., Gannet Hallar, A., McCubbin, I., Thornton, J.A. and Cziczo, D. (2013). Aerosol Measurements at a High-Elevation Site: Composition, Size, and Cloud Condensation Nuclei Activity. *Atmos. Chem. Phys.* 13: 11839–11851.

García, M., Rodríguez, S., González, Y. and García, R. (2014). Climatology of New Particle Formation at Izaña Mountain GAW Observatory in the Subtropical North Atlantic. *Atmos. Chem. Phys.* 14: 3865–3881.

Guenther, A., Karl, T., Harley, P., Wiedinmyer, C., Palmer, P. and Geron, C. (2006). Estimates of Global Terrestrial Isoprene Emissions Using Megan (Model of Emissions of Gases and Aerosols from Nature). *Atmos. Chem. Phys.* 2006. 6: p. 3181–3210.

Hallar, A.G., Lowenthal, D.H., Chirokova, G., Borys, R.D. and Wiedinmyer, C. (2011). Wiedinmyer, Persistent Daily New Particle Formation at a Mountain-top Location. *Atmos. Environ.* 45: 4111–4115.

Hallar, A., Lowenthal, D.H., Clegg, S.L., Samburova, V., Taylor, N., Mazzoleni, L.R., Zielinska, B.K., Kristensen, T.B., Chirokova, G. and McCubbin, I.B. (2013). Chemical and Hygroscopic Properties of Aerosol Organics at Storm Peak Laboratory. *J. Geophys. Res.* 118: 4767–4779, doi: 10.1002/jgrd.50373.

Hõrrak, U., Salm, J. and Tammet, H. (2000. Statistical Characterisation of Air Ion Mobility Spectra at Tahkuse Observatory: Classification of Air Ions. *J. Geophys. Res.* 105: 9291–9302.

Jaatinen, A., Hamed, A., Joutsensaari, J., Mikkonen, S., Birmili, W., Wehner, B., Spindler, G., Wiedensohler, A., Decesari, S., Mircea, M., Facchini, M.C., Junninen, H., Kulmala, M., Lehtinen, K.E.J. and Laaksonen, A. (2009). A comparison of New Particle Formation Events in the Boundary Layer at Three Different Sites in Europe. *Boreal Environ. Res.* 14: 481–498.

Kanawade, V.P., Benson, D.R. and Lee, S.-H. (2012). Statistical Analysis of 4-Year Observations of Aerosol Sizes in a Semi-Rural Continental Environment. *Atmos. Environ.* 59: 2012: 30–38.

Kivekäs, N., Sun, J., Zhan, M., Kerminen, V.M., Hyvärinen, A., Komppula, M., Viisanen, Y., Hong, N., Zhang, Y., Kulmala, M., Zhang, X.C. and Lihavainen, H. (2009). Long Term Particle Size Distribution Measurements at Mount Waliguan, a High-Altitude Site in Inland China. *Atmos. Chem. Phys.* 2009. 9: p. 5461–5474.

Kulmala, M., Toivonen, A., Makela, J.M. and Laasonen, A. (1998). Analysis of the Growth of Nucleation Mode Particles Observed in Boreal Forest. *Tellus Ser. B* 50: 449–462.

Kulmala, M. (2003). How Particles Nucleate and Grow. *Science* 302: 1000–1001.

Lowenthal, D.H., Borys, R.D. and Wetzel, M.A. (2002). Aerosol Distributions and Cloud Interactions at a Mountaintop Laboratory. *J. Geophys. Res.* 107: 4345, doi: 10.1029/2001JD002046, 2002.

Mäkelä, J.M., Dal Maso, M., Pirjola, L., Keronen, P., Laakso, L., Kulmala, M. and Laaksonen, A. (2000). Characteristics of the Aerosolparticle Formation Events Observed at a Boreal Forest Site in Southern Finland. *Boreal Environ. Res.* 5: 299–313.

Merikanto, J., Spracklen, D., Mann, G., Pickering, S. and Carslaw, K. (2009). Impact of Nucleation on Global CCN. *Atmos. Chem. Phys.* 9: 8601–8616.

Neitola, K., Asmi, E., Komppula, M., Hyvärinen, A.-P., Raatikainen, T., Panwar, T., Sharma, V. and Lihavainen, H. (2011). New Particle Formation Infrequently Observed in Himalayan Foothills–Why?. *Atmos. Chem. Phys.* 11: 8447–8458.

Nilsson, E.D. and Kulmala, M. (1998). The Potential for Atmospheric Mixing processes to Enhance the Binary Nucleation Rate. *J. Geophys. Res.* 103: 1381–1389.

Nilsson, E.D., Pirjola, L. and Kulmala, M. (2000). The Effect of Atmospheric Waves on Aerosol Sucleation and Size Distribution. *J. Geophys. Res.* 105: 19917–19926.

Nilsson, E.D., Paatero, J. and Boy, M. (2001). Effects of Air Masses and Synoptic Weather on Aersol Formation in the Continental Boundary Layer. *Tellus Ser. B* 53: 462–478.

Oberdörster, G., Ferin, J., Gelein, R., Soderholm, S.C. and Finkelstein, J. (1992). Role of the Alveolar Macrophase in Lung Injury-studies with Ultrafine Particles. *Environ. Health Perspect.* 97: 193–199.

Peters, A., Wichmann, H.E., Tuch, T., Heinrich, J. and Heyder, J. (1997). Respiratory Effects are Associated with Number of Ultrafine Particles. *Am. J. Respir. Crit. Care Med.* 155: 1376–1383.

Pryor, S.C., Spaulding, A.M. and Barthelmie, R.J. (2010). New Particle Formation in the Midwestern USA: Event Characteristics, Meteorological Context and Vertical Profiles. *Atmos. Environ.* 44: 4413–4425

Rose, C., Sellegri, K., Velarde, F., Moreno, I., Ramonet, M., Weinhold, K., Krejci, R., Ginot, P., Andrade, M., Wiedensohler, A. and Laj, P. (2015). Frequent Nucleation Events at the High Altitude Station of Chacaltaya (5240 m a.s.l.), Bolivia. *Atmos. Environ.* 102, 2015: 18–29.

Shaw, G.E. (2007). Aerosols at a Mountaintop Observatory in Arizona. *J. Geophys. Res.* 112: D07206.

Spracklen, D.V., Carslaw, K.S., Merikanto, J., Mann, G.W., Reddington, C.L., Pickering, S., Ogren, J.A., Andrews, E., Baltensperger, U., Weingartner, E., Boy, M., Kulmala, M., Laakso, L., Lihavainen, H., Kivekäs, N., Komppula, M., Mihalopoulos, N., Kouvarakis, G., Jennings, S.G., O'Dowd, C., Birmili, W., Wiedensohler, A., Weller, R., Gras, J., Laj, P., Sellegri, K., Bonn, B., Krejci, R., Laaksonen, A., Hamed, A., Minikin, A., Harrison, R.M., Talbot, R. and Sun, J. (2010). Explaining Global Surface Aerosol Number Concentrations in Terms of Primary Emissions and Particle Formation. *Atmos. Chem. Phys.* 4775–4793, 2010.

Stanier, C.O., Khlystov, A.Y. and Pandis, S.N. (2004). Nucleation Events during the Pittsburgh Air Quality Study: Description and Relation to Key Meteorological, Gas Phase, and Aerosol Parameters Special Issue of Aerosol Science and Technology on Findings from the Fine Particulate Matter Supersites Program. *Aerosol Sci. Technol.* 38: 253–264

Twomey, S.A. (1974). Pollution and the Planetary Albedo. *Atmos. Environ.* 8: 1251–1256.

Twomey, S.A., Piepgrass, M. and Wolfe, T.L. (1984). An Assessment of the Impact of Pollution on Global Cloud Albedo. *Tellus Ser. B*. 36: 356–366.

Venzac, H., Sellegri, K., Laj, P., Villani, P., Bonasoni, P., Marinoni, A., Cristofanelli, P., Calzolari, F., Fuzzi, S., Decesari, S., Facchini, M.C., Vuillermoz, E. and Verza, G.P. (2008). High Frequency New Particle Formation in the Himalayas. *Proc. Natl. Acad. Sci. U.S.A.* 105: 15666–15671.

Weber, R.J., McMurry, P.H., Eisele, F. and Tanner, D.J. (1995). Measurement of expected Nucleation Precursor species and 3-500-nm diameter particles at Mauna Loa Observatory, Hawaii. J. Atmos. Sci.,. 52(12): p. 2242–2257.

Weingartner, E., Nyeki, S. and Baltensperger, U. (1999). Seasonal and Diurnal Variation of Aerosol Size Distributions (10<D<750 nm) at a High-alpine Site (Jungfraujoch 3850 m asl). *J. Geophys. Res.* 104: 26809–26820.

Wehner, B., Siebert, H., Ansmann, A., Ditas, F., Seifert, P., Stratmann, F., Wiedensohler, A., Apituley, A., Shaw, R.A., Manninen, H.E. and Kulmala, M. (2010). Observations of Turbulence-induced New Particle Formation in the Residual Layer. *Atmos. Chem. Phys.* 10: 4319–4330.

Yu, F. and Luo, G. (2009). Simulation of Particle Size Distribution with a Global Aerosol Model: Contribution of Nucleation to Aerosol and CCN Number Concentrations. *Atmos. Chem. Phys.* 9: 7691–7710.

Yu, F. (2010). Ion-mediated Nucleation in the Atmosphere: Key Controlling Parameters, Implications, and Look-up Table. *J. Geophys. Res.* 115: D03206, doi: 10.1029/2009JD012630.

Yu, F. andHallar, A.G. (2014). Difference in Particle Formation at a Mountain-top Location during the Spring and Summer: Implications for the Role of Sulfuric Acid and Organics in Nucleation. *J. Geophys. Res.* 119: 12246–12255.

Zhao, Y., Hallar, A.G. and Mazzoleni, L.R. (2013). Atmospheric Organic Matter in Clouds: Exact Masses and Molecular Formula Identification Using Ultrahigh-resolution FT-ICR Mass Spectrometry. *Atmos. Chem. Phys.* 13: 12343–12362, doi: 10.5194/acp-13-12343-2013.

Received for review, May 17, 2015
Revised, August 4, 2015
Accepted, November 5, 2015